Thin Poly(styrene-*block*-4-hydroxystyrene) Block Copolymer Films Spin-Coated Directly on Topographic Prepattern Substrates

Geuntak Lee,[†] Pil Sung Jo,[†] Bokyung Yoon,[†] Tae Hee Kim,[†] Himadri Acharya,[†] Hiroshi Ito,[‡] Ho-Cheol Kim,[‡] June Huh,[§] and Cheolmin Park*,[†]

Department of Materials Science and Engineering, Yonsei University, Seoul 120-749, Korea; IBM Almaden Research Center, 650 Harry Road, San Jose, California 95120; and Department of Materials Science and Engineering, Seoul National University, Seoul 151-742, Korea

Received July 19, 2008; Revised Manuscript Received October 1, 2008

ABSTRACT: We have investigated the formation of *as-cast* thin films of a poly(styrene-*block*-4-hydroxystyrene) (PS-*b*-PHOST) copolymer *spin-coated directly* on topographic prepattern substrates. Either wetting or dewetting of a polymer thin film on the elevated regions occurs in the nonequilibrium state during spin-coating with solvent vapor saturated and strongly depends on the dimensions of the prepatterns. The ratio of periodic unit area to elevated one of a prepattern (β value) is found as one of the most important factors for wettability of a thin film. The dewetting of a thin film, guided by the edges of either elevated individual periodic lines or mesas, took place with self-assembled block copolymer nanostructure when the β value was greater than a critical value of ~4 in our system.

Self-assembled block copolymers present an efficient way for fabricating well-ordered and periodic nanostructures due to thermodynamic energy balance between two competing forces: minimization of interfacial surface area and maximization of chain conformational entropy of the constituent blocks.[1,2] Facile film formation of block copolymers in most cases based on spin-coating imparts additional benefit for many thin film applications such as nanolithographic masks and filtering membranes when combined with various external fields for controlling both orientation and registration of nanodomains.[3] Among diverse techniques for controlling block copolymer self-assembly, quantized spatial registration of nanostructure on a topographical periodic prepattern, known as graphoepitaxy, has been of great interest mainly due to its compatibility with the current semiconductor process technology since its first demonstration by Kramer's group.[4]

A thin block copolymer film in particular on a topographic prepattern has been prepared either by transferring the film spin-coated and subsequently floated on an liquid/air interface to the prepattern or by *directly spin-coating* the film on the prepattern. In the latter case, in general the film formation strongly depends on the shape, height, and size of the individual prepatterns.[5] When film thickness is comparable or less than the trench depth of a prepattern in most of thin block copolymer film formation for graphoepitaxy, spin-coating frequently causes nonuniform film with the thickness on the elevated regions different from that on the recessed ones. For certain conditions, incomplete coverage of a film may occur in particular on the elevated regions, resulting in a film structure reminiscent of dewetting of polymer films. In spite of many theoretical and experimental studies of micron thick polymer film directly spin-coated on topographic micropatterns,[6] direct film formation of a block copolymer upon spin-coating has rarely been reported on prepatterns with hundreds of nanometers in size. It is noteworthy that in spite of very fast kinetics of film formation the self-assembly of these films was in principle caused by polymer mobility in films containing solvent vapors, which is similar to solvent annealing or controlled solvent evaporation.[4]

In this article, we examine the effect of topographic nanopatterns on the formation of *as-cast* thin films of a poly(styrene-*block*-4-hydroxystyrene) (PS-*b*-PHOST) copolymer by spin-coating. Utilization of self-assembled block copolymers was additionally beneficial because the orientation of block copolymer microdomains developed with respect to patterned surface allowed us indirectly to evaluate the local thickness of polymer film.[7] In particular, we modified our spin-coater such that solvent vapor was saturated during film formation, which provided sufficient time and chain mobility for the block copolymer to recognize the topology of a prepattern upon fast spin coating (Supporting Information, Figure S1). The solvent vapor was also helpful for fully developing phase-separated microstructure of the block copolymer in the film.

A series of periodic 1D line patterns were fabricated by conventional optical lithography technique using 193 nm photoresist and subsequent etching with CF_4 plasma and are shown with the various crest and periodicity in Table 1. The depth of trenches is fixed as ~45 nm for all prepatterns, and the contact angle of water on the prepatterns was all ~43°. Before direct spin-coating of an asymmetric PS-*b*-PHOST with the number-average molecular weight (M_n) of 67 800 g/mol prepared and supplied by Nippon Soda Co., Ltd., Japan (the volume fraction of PS: 0.37 by ^{13}C NMR; PDI: 1.112 by size exclusion chromatography), an optimized film thickness of PS-*b*-PHOST was first determined to be appropriate for investigating the effect of the topographic patterns. Approximately 10 nm thick PS-*b*-PHOST film was obtained from 1 wt % solution dissolved in propylene glycol monomethyl ether acetate (PGMEA) on a (100) Si wafer with native oxide by spin-coating under saturated solvent vapor, as determined by ellipsometry (SE MG-1000 Nanoview Co.). The surface height variation induced during spin-coating is large enough to directly observe the nanostructure in AFM, consistent with the results by Bosworth et al.[8] Both AFM image and X-ray scattering results show that well-defined cylindrical PS microdomains are aligned parallel to the substrate with approximately 40 and 20 nm in

* Corresponding author: Tel +82-2-2123-2833, Fax +82-2-312-5375, e-mail cmpark@yonsei.ac.kr.
[†] Yonsei University.
[‡] IBM Almaden Research Center.
[§] Seoul National University.

10.1021/ma801631y CCC: $40.75
Published on Web 11/06/2008

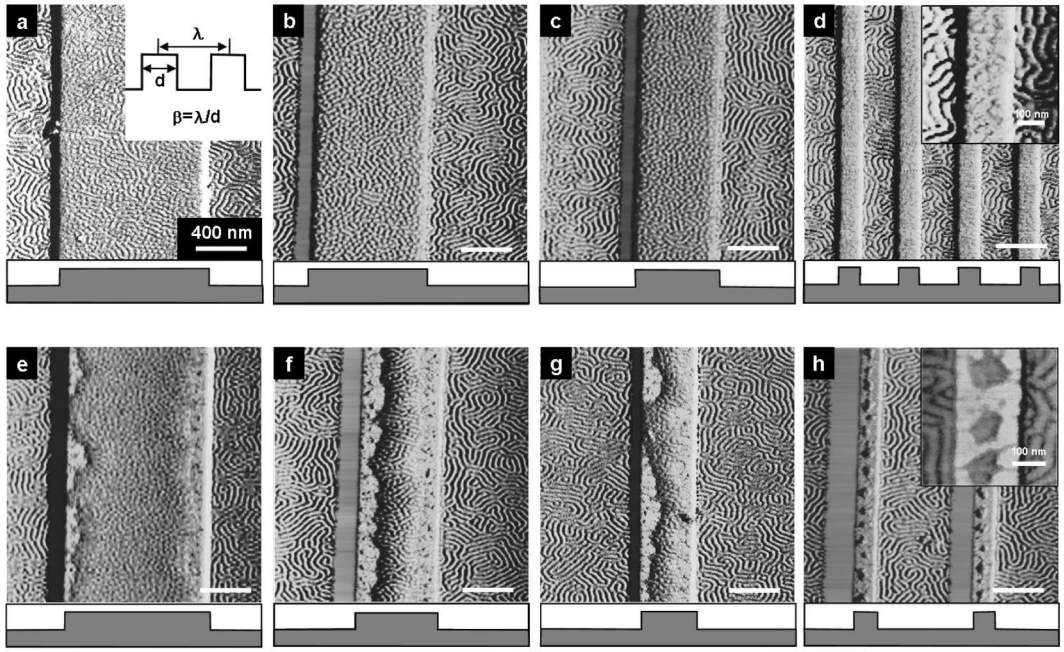

Figure 1. Tapping mode AFM images in phase contrast of PS-*b*-PHOST thin films formed on 1D topographic line patterns. The schematic pattern profile is illustrated below each image. (a), (b), (c), and (d) correspond to the prepatterns of 5, 4, 3, and 1 in group I of Table 1, respectively. (e), (f), (g), and (h) correspond to the prepatterns of 11, 9, 8, and 7 in group II of Table 1, which show all the incomplete wetting of block copolymer films. The inset of (a) schematically defines the β value. A magnified image of (d) in the inset exhibits homogeneous film formed on the crests. Isolated dewetted domains with the characteristic stretched arms are clearly visible in the inset of (h).

Table 1. Characteristics of Thin PS-*b*-PHOST Copolymer Films Formed via Spin-Coating on Various Topographic Line Patterns[a]

	group I						group II						group III		
prepatterns	1	2	3	4	5	6	7	8	9	10	11	12	13	14	15
crest width (d)/nm	120	370	630	860	1070	2100	140	400	600	840	1000	2100	600	1300	2000
periodicity (λ)/nm	350	800	1260	1720	2140	4100	820	1700	2600	3510	4160	8600	800	1650	2600
β (λ/d)	2.92	2.16	2.00	2.00	2.00	1.95	5.86	4.25	4.33	4.18	4.16	4.10	1.33	1.27	1.30
film on crest	wet	wet	wet	wet	wet	wet	dewet	dewet	dewet	dewet	slightly dewet	slightly dewet	wet	wet	wet
area fraction (A/A_0)	1	1	1	1	1	1	0.32	0.54	0.50	0.56	0.90	0.95	1	1	1

[a] Films are all completely and homogeneously wet on pattern trenches. The height of all prepatterns is ~45 nm.

periodicity and diameter, respectively (Supporting Information, Figure S2). We speculated the formation of half PS cylinders aligned parallel to the substrate. The effect of the saturated solvent vapor was apparent because a film prepared without saturated vapor did not show distinct cylindrical PS microdomains. Selective wetting of PHOST block to the substrate and PGMEA vapor which is preferential to PHOST induce an asymmetric boundary condition at the PS-*b*-PHOST/air interface, giving rise to PS cylinders aligned parallel to the substrate, as also confirmed by grazing incidence small angle X-ray scattering (Supporting Information, Figure S2). It is noted that a film prepared with the saturated vapor becomes thinner even under the same spin-coating condition than one without vapor of ~20 nm in thickness. The reason for the thinner film formation with saturated vapor is possibly because the solvent vapor allows the film to remain fluid longer, and thus spin-coating process can throw off more of the fluid.

First, we investigated the effect of line width of crest regions on thin PS-*b*-PHOST film formation using a series of prepatterns denoted as group I in Table 1 which all have the ratio of periodicity of a pattern (λ) to crest width (d) (β value) of 1.95−2.92. A homogeneous flat film was formed both on crest and trench with all the patterns investigated. Typical examples of the spin-coated films are shown on the prepatterns in Figure 1a−d. Even in a prepattern with the crest of 120 nm, a flat film was obtained in Figure 1d, which implies that absolute crest width is not so much sensitive to destabilizing a film. The fact that PS cylinders oriented perpendicular to the surface are dominantly developed on the elevated regions while in-plane cylinders formed on the recessed ones implies that the film on the crest is thinner in thickness than that on the trench,[7] also consistent with the results with homopolymers predicted both by theoretical models and experiments.[6] The measured thickness of a film was ~6 nm with the perpendicular PS cylinders on a flat surface.

Another set of prepatterns (group II) was examined on film formation with various β values in Table 1. As noted, the width of crests ranges from 140 nm to 2 μm, similar to that of the group I patterns. The β values of group II are from 4.10 to 5.86 as indicated in Table 1. Obviously, a film became destabilized on the prepatterns and dewetting occurred in particular at the elevated regions as shown in Figure 1e−h. It is apparent that the dewetting was preferentially initiated at the sharp pattern edges of the crests. Directly compared with Figure 1a,c, the films in Figure 1e,f obviously dewet even on the prepatterns with the similar crest width, respectively. In addition, a pattern with crest and pattern periodicity of 140 and 820 nm, respectively, induces the most severe dewetting of a PS-*b*-PHOST film, leading to an intriguing microstructure in which isolated dewetted domains with ~80 nm in size are regularly aligned along the line as shown in Figure 1h and the inset. This result at the same time suggests a fast and facile technique for fabricating an ordered nanostructure based on spontaneous

dewetting of a polymer film without further thermal or solvent treatment.

Our results clearly show that (1) dewetting of a PS-*b*-PHOST film occurs preferentially at the sharp edge regions of topographic lines and (2) a prepattern with larger β value tends to be more favorable for destabilizing a film regardless of the absolute dimension of either crest or trench. The dewetting at the sharp edge of the topographic prepatterns is well understood by the previous work including our recent study where dewetting of PS thin film spin-coated on a topographic prepattern was initiated preferentially at the pattern edges during thermal treatment.[9] Localized polymer flow at the pattern edges resulted in the preferential dewetting of PS films in order to spontaneously reduce the excess chemical potential induced by high curvature at the pattern edge.[9] We analyzed the surface profiles of the AFM images of the PS-*b*-PHOST films as a function of the β values in relation to the bare substrates. As expected, the film thickness at the edge region became thinner than at the center with the β value close to 4, which evidence that the film breakup preferentially occurs at the edges (Supporting Information, Figure S3). In the current system, the unique dewetted structure of PS-*b*-PHOST film was additionally developed with the characteristic stretched and torn branches of the film at the pattern boundaries in Figure 1e−h and in particular the inset of Figure 1h. The structure was attributed to the anchoring effect of HOST blocks on the surface mainly due to a very strong hydrogen bonding interaction between hydroxyl moiety of HOST blocks and hydrophilic oxide pattern surface.[10]

Considering the fact that all prepatterns used is the same chemical nature with the same height of 45 nm, the dewetting of PS-*b*-PHOST film becomes strongly affected with the β values. It is also noted that the resulting films on crest regions are all similar in thickness regardless of β value, based on the microstructure of PS cylinders aligned perpendicular to the surface for all the prepatterns. In fact, the prepatterns resulting in the dewetting of PS-*b*-PHOST films have the β values greater than ~4. In order to confirm our speculation, we introduced a different set of line patterns as group III in Table 1 whose β values are all less than 2 with crest width much larger than that of trenches. Again crest width varies from 2 μm to 600 nm and is similar to that of either group I or II. The prepatterns gave rise to homogeneous films formed both on the crests and the trenches without dewetting (Supporting Information, Figure S4).

The complicated submicron thick film formation over topography has been greatly investigated during spin-coating which involves the competition of three major driving fields of surface tension, viscosity of a solution, and shrinking speed.[6g] The planarization of a film on a topographic surface renders the film on crest regions thinner than on trenches and is proportional to surface tension and inversely proportional to both viscosity and shrinking speed with a parameter of ratio [(surface tension/{(viscosity) × (shrinking speed)}]. Further planarization of ca. 10 nm thick film on a topology with 45 nm height in our case gave rise to the incomplete wetting of the thinner film on the elevated crest regions as shown in Figure 1e−h. The shape of the liquid solution surface during spin-coating must be maintained if the crests are not to be dewetted. Dewetting is ultimately caused by the draining of fluid from the crests to the trenches. The driving force for this draining is capillarity. That is, the positive curvature on top of the crest drives flow into the trench. It is clear that curvature is initially large if both d and λ are small with low β values. The capillary pressure-driven flow will rapidly tend to raise the thickness of the solution in the trenches, thus reducing the curvature difference and the driving capillary pressure. However when β is large, the decrease in driving capillary pressure with flow of solution is much less, giving rise to such a thin solution film near the edge of the crest that it will eventually dewet.

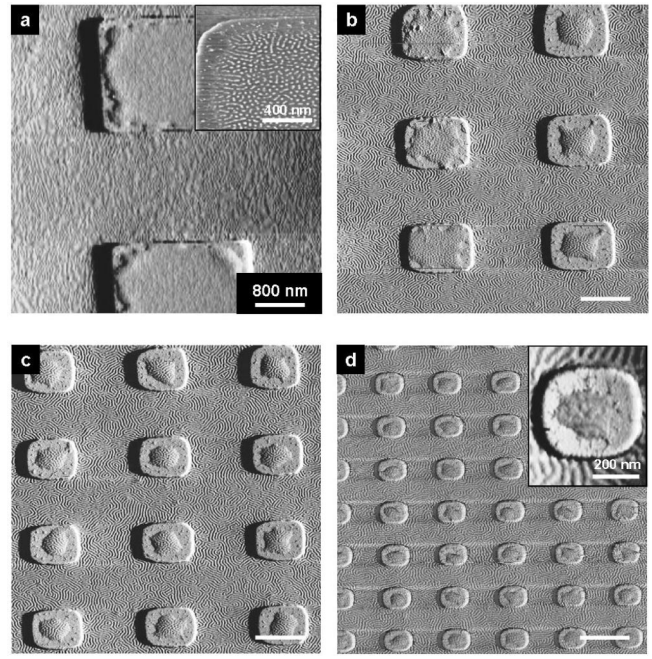

Figure 2. Tapping mode AFM images in phase contrast of PS-*b*-PHOST thin films formed on 2D topographic square mesas arrayed into *square* symmetry with various mesa size and periodicity. All square patterns with the periodicity/mesa size of (a) 4400/2200 nm, (b) 2140/1070 nm, (c) 1660/830 nm, and (d) 750/340 nm induce incomplete wetting of the films on the mesa regions. Inset of (a) is a magnified image of (a) with PS cylinders vertically ordered on the surface.

In addition to the effect of curvature difference, we presume that the orientation of cylinder nanostructure also plays a role in the wetting behavior. The strong affinity of PHOST to the surface of topographic pattern due to hydrogen bonding with native oxide layer favorably forms the in-plane PS cylinders in the recessed region where the film thickness is thick enough to accommodate the periodicity of in-plane half-cylinders. On the other hand, the orientation of cylinder in the elevated region is perpendicular to the substrate because the film thickness is too thin to accommodate in-plane cylinder, as seen in Figure 1. We expect that the contribution of long-range van der Waals force stabilizes the structured fluid forming in-plane half-cylinder in a trench more than does the fluid of perpendicular cylinder on the top of the crest because of not only trench shape but also cylinder orientation. In this scenario, when dewetting occurs, the surface energy increase by exposing the substrate on the top of elevated region should be rewarded by the long-range van der Waals contribution with the favorable in-plane half-cylinder orientation in the recessed region. Therefore, when β is large such that the trench is wide and the diameter of a mesa is small, the fluid desires to fall into the trench, which results in the dewetting on the top of crest.

The PS-*b*-PHOST film formation on prepatterns with tetragonal arrays of square mesas in addition supports our argument with the influence of the β value as shown in Figure 2. On the square mesas with the size ranging from 2 μm to 340 nm, it is apparent that PS-*b*-PHOST films all dewetted with the cylindrical microdomains perpendicular to the surface. The

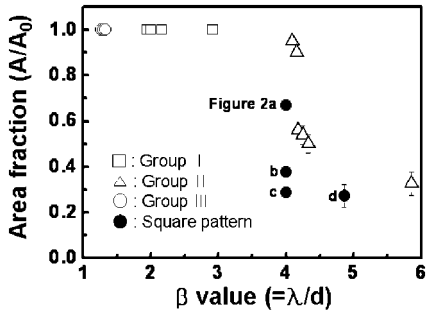

Figure 3. Plot of the area fraction covered with PS-*b*-PHOST film per unit cell area (d^2) of a prepattern as a function of the β values. The dewetting of a film occurs with the β value greater than ~4 for both line and square patterns although the area fraction becomes significantly lower for the square patterns.

dewetting, again initiated at the mesa edges, becomes more dominant with the mesa of 340 nm in size in Figure 2d. To correlate the results of the 2D mesa arrays with those from the previous 1D line patterns, we calculated the ratio of the periodic tetragonal unit cell area to the mesa one which is the β values for 2D patterns and examined the effect of the ratios on dewetting of PS-*b*-PHOST film. The ratios calculated are all 4 except the pattern of Figure 2d, which has the ratio of 4.85. Consistent with the results with 1D line patterns in which the patterns with the β values greater than ~4 induced the preferential dewetting, the 2D patterns with the large ratios also gave rise to the dewetting of the block copolymer. In particular, the dewetting occurred more severely on the 340 nm pattern with the ratio of 4.85. The dewetted structures of PS-*b*-PHOST films formed on various prepatterns were very stable even after either solvent or thermal annealing for 12 h mainly due to the strong anchoring by hydroxyl group of HOST blocks on native Si oxide surface (Supporting Information, Figure S5).

We quantified the PS-*b*-PHOST film formation on the elevated topographic regions by calculating the averaged film coverage per unit elevated area of a prepattern. Complete wetting of a film on either crest or mesa leads to the fraction of 1, which decreases in proportion with the degree of dewetting. Figure 3 shows a plot of the area fraction as a function of the β values of the prepatterns. It is apparent that the dewetting of a PS-*b*-PHOST film was significantly promoted by β values in particular greater than ~4 in our experimental conditions. The 1D prepatterns of group I and III in Table 1 with the β values lower than 4 exhibit complete wetting of the elevated regions while the prepatterns of group II with the β values greater than 4 clearly gave rise to the dewetting of a film.

We also plotted the fraction of dewetted film on mesas based in Figure 2. A similar tendency was observed in which the β values greater than ~4 resulted in dewetting of the block copolymer on mesas as shown in Figure 3. Compared with the results from the 1D line patterns, the dewetting on the 2D mesas prevails more at a constant β value, which may be due to the different geometry of the prepatterns. The square shaped edge of 2D mesas seems to be more strongly affected during rapid rotation of a substrate in spin-coating even with the same edge length per unit area as that of a 1D line pattern. In addition, we employed a different set of prepatterns with the height of ~200 nm in order to examine the effect of the pattern height on the film formation of PS-*b*-PHOST. The β value dependence was also observed of PS-*b*-PHOST dewetting on the prepatterns. Interestingly, however, the dewetting on elevated region occurred even on a prepattern with the β value of ~2 (Supporting Information, Figure S6). The dewetting also depends on a film thickness as confirmed with the thicker film from 2 wt % solution on the prepatterns. The thicker films did not induce the dewetting but edge thinning at the edges of a prepattern with the β value of 4. It is noted that the degree of ordering of PS cylinders remained almost same as a function of film thickness.

We also examined the topographic effects with homopolymers: PS and PHOST independently. Unfortunately, in our current experimental conditions, we did not observe the dewetting behavior dependent upon the pattern dimensions with the homopolymers. For PS films, the dewetting always occurred regardless of the prepatterns due to its large surface energy difference with Si substrate. On the other hand, homogeneous, flat PHOST films were obtained on all the prepatterns used in the current work because of its good interaction with the substrate. We do still believe that the lateral aspect ratio dependent dewetting observed in the PS-*b*-PHOST copolymer is not unique but general to any thin polymer films. A system, however, requires more delicate adjustment of the experimental parameters such as surface energies of solvent, substrate, and polymers and dimension of prepatterns.

We systematically investigated the effect of topographic pattern dimension on film formation of a cylinder forming PS-*b*-PHOST copolymer in rapid spin-coating under saturated solvent vapor. Our results clearly indicate that the ratio of periodic unit cell to elevated part, characterized by the β value ($= \lambda/d$), is one of the most important factors to determine the wettability of the film. In our experimental conditions, the prepatterns with the β values greater than ~4 gave rise to the incomplete wetting of a film which preferentially occurred at the edges of the elevated regions.

Acknowledgment. This work was supported by National Research Program for Memory Development sponsored by Korea Ministry of Knowledge and Economy. The X-ray experiments at PAL (4C2 beamline). Korea, were supported by MOST and POSCO, Korea. This work was supported by the Second Stage of Brain Korea 21 Project in 2008, Seoul Science Fellowship, Seoul Research and Business Development Program (10801) and the Korea Science and Engineering Foundation (KOSEF) grant funded by the Korea government (MEST)(No. R11-2007-050-03001-0).

Supporting Information Available: Schematic of block copolymer film preparation, AFM image and grazing incidence small angle scattering pattern of PS-*b*-PHOST, surface profiles of AFM image of PS-*b*-PHOST, and tapping mode AFM images of PS-*b*-PHOST films. This material is available free of charge via the Internet at http://pubs.acs.org.

References and Notes

(1) Hamley, I. W. *Angew. Chem., Int. Ed.* **2003**, *42*, 1692.
(2) Ruzette, A.-V.; Leibler, L. *Nat. Mater.* **2005**, *4*, 19.
(3) Park, C.; Yoon, J.; Thomas, E. L. *Polymer* **2003**, *44*, 6725.
(4) (a) Segalman, R. A.; Yokoyama, H.; Kramer, E. J. *Adv. Mater.* **2001**, *13*, 1152. (b) Kim, S. O.; Solak, H. H.; Stoykovich, M. P.; Ferrier, N. J.; de Pablo, J. J.; Nealey, P. F. *Nature (London)* **2003**, *424*, 411. (c) Cheng, J. Y.; Mayes, A. M.; Ross, C. A. *Nat. Mater.* **2004**, *3*, 823. (d) Sundrani, D.; Darling, S. B.; Sibener, S. J. *Nano Lett.* **2004**, *4*, 273. (e) Stoykovich, M. P.; Müller, M.; Kim, S. O.; Solak, H. H.; Edwards, E. W.; de Pablo, J. J.; Nealey, P. F. *Science* **2005**, *308*, 1442. (f) Black, C. T. *Appl. Phys. Lett.* **2005**, *87*, 163116. (g) Park, S −M.; Stoykovich, M. P.; Ruiz, R.; Zhang, Y.; Black, C. T.; Nealey, P. F. *Adv. Mater.* **2007**, *19*, 607. (h) Rockford, L.; Liu, Y.; Mansky,

P.; Russell, T. P. *Phys. Rev. Lett.* **1999**, *82*, 2602. (i) Kim, S. H.; Misner, M. J.; Xu, T.; Kimura, M.; Russell, T. P. *Adv. Mater.* **2002**, *16*, 226. (j) Jung, Y. S.; Ross, C. A. *Nano Lett.* **2007**, *7*, 2046.

(5) Luo, C.; Xing, R.; Zhang, Z.; Fu, J.; Han, Y. *J. Colloid Interface Sci.* **2004**, *269*, 158.

(6) (a) Bornside, D. E. *J. Electrochem. Soc.* **1990**, *137*, 2589. (b) Manske, L. M.; Graves, D. B.; Oldham, W. G. *Appl. Phys. Lett.* **1990**, *56*, 2348. (c) Sukanek, P. C. *J. Electrochem. Soc.* **1991**, *138*, 1712. (d) Peurrung, L. M.; Graves, D. B. *J. Electrochem. Soc.* **1991**, *138*, 2115. (e) Peurrung, L. M.; Graves, D. B. *IEEE Trans. Semi. Manuf.* **1993**, *6*, 72. (f) Gu, J.; Bullwinkel, M. D.; Campbell, G. A. *J. Electrochem. Soc.* **1995**, *142*, 907. (g) Hirasawa, S.; Saito, Y.; Nezu, H.; Ohashi, N.; Maruyama, H. *IEEE Trans. Semi. Manuf.* **1997**, *10*, 438.

(7) Knoll, A.; Horvat, A.; Lyakhova, K. S.; Krausch, G.; Sevink, G. J. A.; Zvelindovsky, A. V.; Magerle, R. *Phys. Rev. Lett.* **2002**, *3*, 35501.

(8) Bosworth, J. K.; Paik, M. Y.; Ruiz, R.; Schwartz, E. L.; Huang, J. Q.; Ko, A. W.; Smilgies, D.-M.; Black, C. T.; Ober, C. K. *ACS Nano* **2008**, *2*, 1396.

(9) Yoon, B.; Acharya, H.; Lee, G.; Kim, H.-C.; Huh, J.; Park, C. *Soft Matter* **2008**, *4*, 1467.

(10) Yoon, B.; Huh, J.; Ito, H.; Frommer, J.; Sohn, B.-H.; Kim, J. H.; Thomas, E. L.; Park, C.; Kim, H.-C. *Adv. Mater.* **2007**, *19*, 3342.

MA801631Y